Modelling of necking during creep of grade 91 steel

R. Lim, Maxime Sauzay, F. Dalle, I. Tournié, Anne-Françoise Gourgues-Lorenzon

MODELLING OF NECKING DURING CREEP OF GRADE 91 STEEL

R. Lim[1)], M. Sauzay[1)], F. Dalle[1)], I. Tournié[1)], A.F. Gourgues-Lorenzon[2)]
[1)] CEA Saclay, DEN/DMN/SRMA, 91191 Gif-sur-Yvette, France
[2)] MINES ParisTech/Centre des Matériaux UMR CNRS 7633, BP 87, 91003 Evry, France

ABSTRACT

This paper addresses a necking model used for predicting creep lifetimes of Grade 91. Creep results from more than 15 tests at 500-600°C on Grade 91 are used. One of them fractured after 160×10^3h at 500°C. Hart's necking model using the Norton power-law rule correctly predicts lifetimes up to 60×10^3h at 500°C. However, it overestimates lifetimes in all other loading conditions. The necking model including material creep softening, appearing during the tertiary stage, predicts lifetimes differing from the experimental results by less than 20% for lifetimes up to 160×10^3h at 500°C and 50% up to 94×10^3h at 600°C. These predictions are reasonable with respect to experimental scatter. The model predicts the time evolution of the necking section in agreement with an interrupted creep test at least up to 75% of the experimental lifetime. Two lifetime predictions are deduced from this necking model. For a large number of tempered martensitic steels, these two criteria bound the experimental lifetimes up to 200×10^3h at 500-700°C.

KEYWORDS

creep, Grade 91 steel, tertiary stage, softening, necking, lifetime

INTRODUCTION

It is widely believed that modified 9Cr-1Mo (Grade 91) tempered martensite steel is an appropriate material for structural components subjected to high temperature creep, such as coolant pipes of the future power plant-GEN IV. Its mechanical properties are studied in [1].

The Hoff model [2] based on a homogenous reduction in cross-section predicts a creep lifetime which is inversely proportional to the minimum strain rate. This model gives only accurate predictions for short lifetimes but leads to an overestimation of long lifetimes [3]. In fact, the Grade 91 steel softens during creep due to microstructural evolution [4] and such softening increases with increasing lifetime [5]. Hart's necking model [6] using the Norton power law allow predictions of the evolution of the necking section with time. However, for Grade 91 steel, softening occurring during creep should be introduced in the viscoplastic flow rule i.e. a simple Norton-like law cannot be used.

This paper presents creep data corresponding to more than 15 tests on Grade 91 at temperatures between 500 and 600°C. Several necking models are used for lifetime predictions. Experimental results were first used to identify the parameters of two viscoplastic flow rules. The first one is the Norton law leading to the minimum creep strain rate and the second one describes the creep softening behaviour. One interrupted creep test was performed at 500°C and 350 MPa with repeated measurements of the specimen diameter profile. Hart's necking model was applied to this test together with both viscoplastic flow rules. The predicted lifetimes and evolution of the necking section with time are compared to experimental results. Analytical expressions of lifetimes are finally deduced in the form of Monkman-Grant criteria.

MATERIAL, SPECIMEN AND TESTING

The chemical composition and heat treatment of the modified 9Cr-1Mo steel used for the creep tests are given in [3]. All creep tests were carried out at constant temperature (500°C, 550°C and 600°C) and load using specimens of 85mm in length, 40mm in gauge length and 5mm in gauge diameter [3].

One additional multiple-loading-unloading creep test was performed at 500°C and 350MPa. This test includes interruptions and unloading at three different strain levels: 1.68%, 6.8%, and 10%. The diameter profile of the gauge part along the loading axis was measured using a Laser Scan Micrometer, before beginning the test and after each unloading step; then, the specimen was carefully mounted on the creep machine to begin or to continue the creep test until next interruption.

Engineering stress (MPa)	Interrupted points	Engineering strain (%)	Time (h)
350	1	1.68	14
	2	6.80	39
	3	10.00	43
	(fracture)	13.25 (last recorded)	46.4

Table 1: creep test carried out at 500°C and 350MPa on the same Grade 91 steel as in [3], with interruptions at three different strain levels before fracture.

ANALYSIS OF EXPERIMENTAL RESULTS

Creep curves are classically divided into three main stages: primary, secondary, and tertiary stage [7]. The secondary stage covers the time interval during which the creep rate is almost constant and identified by a straight line in the strain vs. time plot. This identification also allows the determination of the time fraction of the tertiary stage i.e. the ratio of the tertiary stage duration to the total creep lifetime. For a given material and temperature this fraction seems to decrease with increasing lifetime. The tertiary time fraction of Grade 91 ranges between 20% (long-term tests) and 70% (short-term tests) at temperatures between 500 and 625°C. The tertiary stage time fractions of Grade 91 are similar to the ones of the Aluminium alloy A5052-0, Grade 92 steel, austenitic stainless steel 316, and Nickel-based alloy IN100. This large tertiary stage time fraction could be attributed to different phenomena, such as necking and softening due to metallurgical evolution.

The true (logarithmic) strain, ε, is calculated from the engineering strain, ε^{eng}, measured during creep tests. True strain rate vs. true strain curves are plotted in Figs 1a-c. The true strain rate reaches its minimum at a strain ranging between 0.6 and 2.5% for temperatures between 500 and 600°C. The coefficients of the Norton power-law equation, Eq. (1), are fitted using minimum true strain rates, $\dot{\varepsilon}_{min}$ (h^{-1}), and applied engineering stresses, σ^{eng} (MPa), of creep tests. Norton parameters (N, C(1/h)) are found to be (20.35, $1.556\ 10^{-55}$), (16.76, $6.967\ 10^{-45}$) and (9.94, $8.418\ 10^{-30}$) respectively at 500, 550°C and 600°C.

$$\dot{\varepsilon}_{min} = C(T)(\sigma^{eng})^{N(T)} \quad (1)$$

After reaching its minimum, the true strain rate accelerates, apparently following an exponential function of the true strain until 50% of the fracture strain (Figs 1a-c). This acceleration is characterized by a softening slope, k. This is in agreement with the results of [8] based on comparisons between creep tension and compression tests (i.e. without any damage cavities). Fig. 1d shows that the value of k increases with decreasing the minimum true strain rate or, equivalently, with increasing lifetime. Thus, the softening slope (k) is phenomenologically represented by Eq. (2), with coefficients (A,α) given by (15.27,0.1098).

$$k = A\left(\dot{\varepsilon}_{min}\right)^{-\alpha} \quad (2)$$

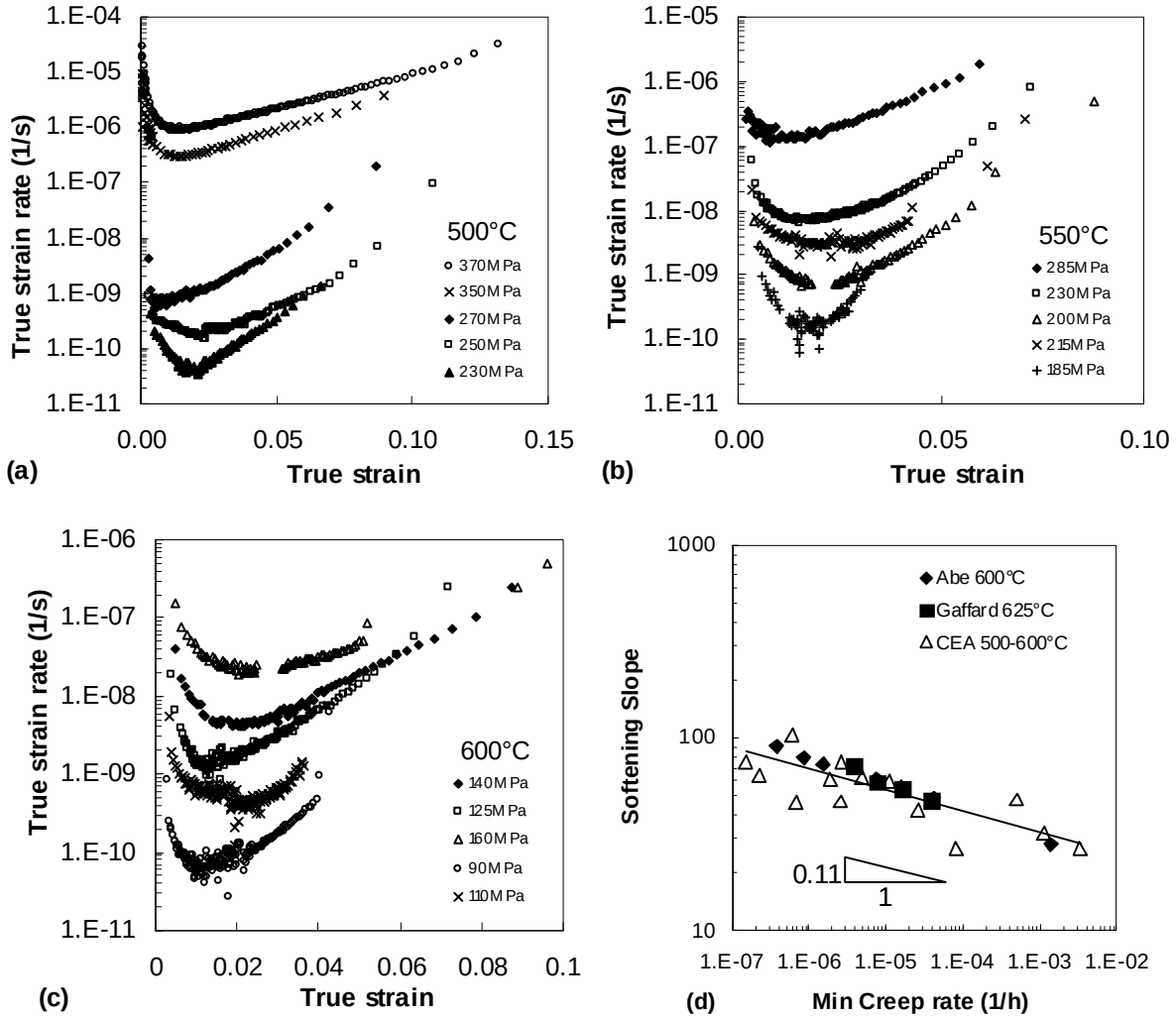

Fig. 1: (a-c) true strain rate acceleration induced by softening, (d) softening slope following minimum creep rate. “Abe 600°C” from [9], “Gaffard 625°C” from [10].

Fig. 2a shows the time evolution of the engineering strain during the interrupted creep test lasting 46h for a stress of 350MPa at 500°C. The lifetime of this test only slightly differs from another test (38h) performed in the same loading conditions. Before the creep test, the roughness on the specimen surface induced a maximum variation of 20μm on the gauge diameter. Until the second interruption (strain of 6.8%) the reduction in cross-section did not appears clearly with eye observation. However, quantitative measurements revealed a 9% reduction at the minimum cross-section (Fig. 2 b). Necking appears clearly only at the third interruption, during which the reduction in cross-section reaches 16%. Finally, the specimen fractured when the reduction in cross-section reaches 82%. This is in agreement with fracture of short-term tests of Grade 91 at temperature ranging in 500-600°C where the reduction in cross-section reaches 80% in average [3]. For long-term tests at 500-600°C on Grade 91, the reduction in cross-section reaches about 20% at fracture [3].

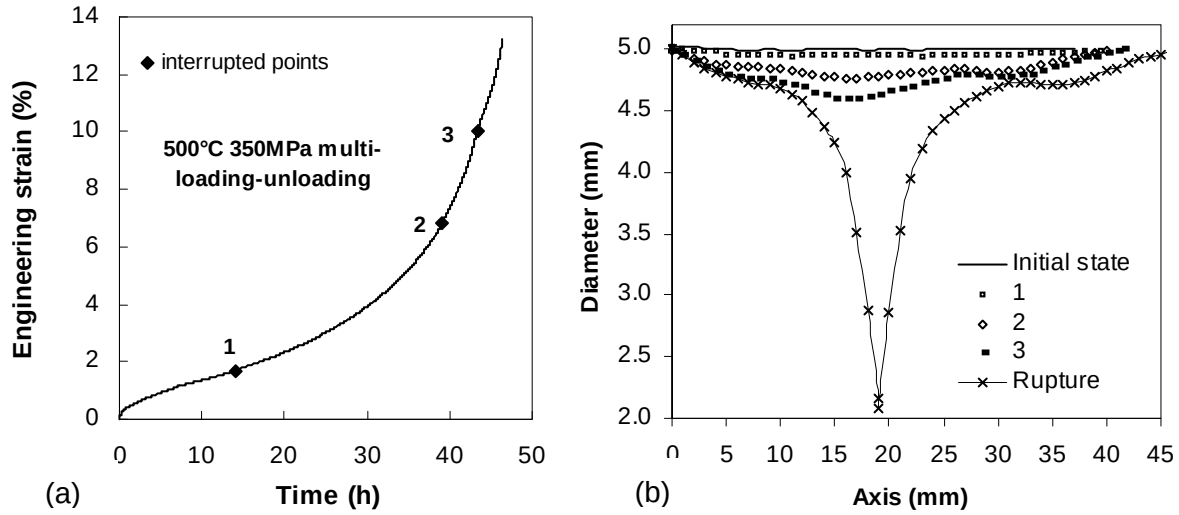

Fig. 2: Interrupted creep test performed at 500°C and 350MPa, (a) creep curve, (b) specimen diameter along axis measured at each interruption.

NECKING MODEL

Prediction of the onset of necking

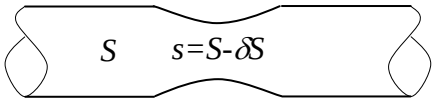

Fig. 3: specimen profile during deformation instability.

At any given time, a small portion of the gauge length is assumed to have a cross-section differing by a small amount, δS, from the remainder which is supposed to have a homogenous cross-section, S. No coupling between both parts is assumed i.e. each part is allowed to deform independently, so that loading remains uniaxial. According to Hart's definition [6], the deformation is unstable if this difference in cross section increases. Using then volume conservation (and assuming no cavitation), Eq. (3), the deformation instability criterion i.e. onset of necking is given by Eq. (4).

$$\dot{\varepsilon} = -\dot{S} / S \tag{3}$$

$$\ddot{\varepsilon}^{eng} / \dot{\varepsilon}^{eng} - 2\dot{\varepsilon}^{eng} / (1+\varepsilon^{eng}) > 0 \tag{4}$$

From experimental creep curves, Eq. (4) allows predictions of the time and strain at which necking starts, $t_{necking}$. However, the measured engineering strains are scattered which causes derivative discontinuities. This is solved by using a sixth-order polynomial regression to fit the experimental ε^{eng} vs. time curves. Using of a forth- or fifth-order polynomial regression leads to a relative change of predictions lower than 10%. In order to keep as accurate as possible, only the sixth-order polynomial regression is used.

The results are given in Fig. 4. Necking is predicted to begin just after the time corresponding to the minimum creep rate. From an experimental point of view, however, macroscopic necking develops significantly only just before fracture (Fig. 2b).

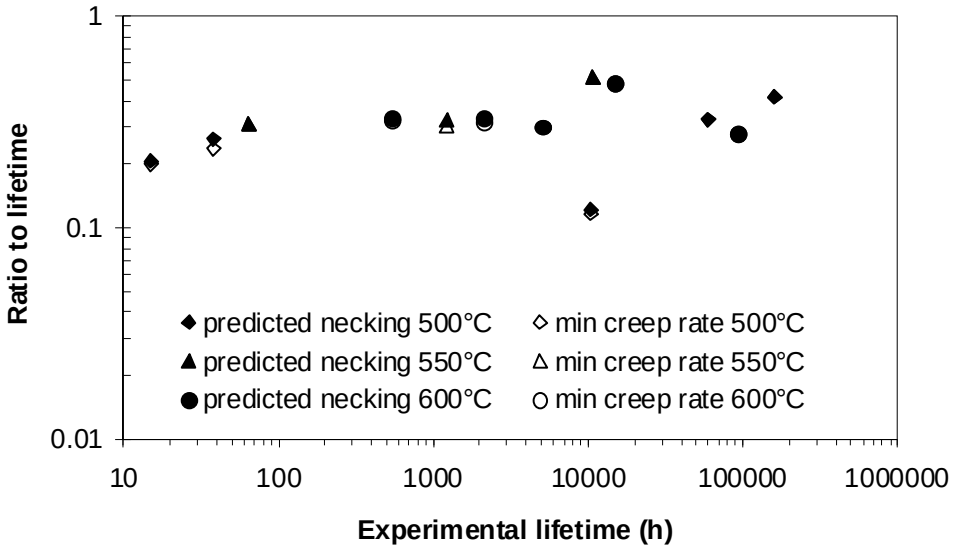

Fig. 4: Predicted times at onset of necking and at minimum creep rate vs. creep lifetime.

Further evolution of necking section during creep

Evaluations of axial stress on necked specimens with notch geometry according to diameter measurements using classical Bridgman plasticity analysis show that the axial stress varies by less than 10% across the necked section. In the model, the stress is assumed to be uniform across the necking cross-section. Thus, the specimen is divided into three parts having uniform cross-sections, S at the two homogenous parts and $s = S-\delta S$ the necking part (Fig. 3).

We suppose that the Norton power-law could be expressed vs. true stress, σ (instead of σ^{eng}) with constant $C^m = C/(1+\varepsilon^{eng})^N$ to simulate creep flow during the tertiary stage:

$$\dot{\varepsilon} = C^m \sigma^N \tag{5}$$

The combination of Eq. (3) and Eq. (5) leads to Eq. (6) giving the homogenous cross-section, in which $S_{necking}$ is respectively the cross-section at time $t_{necking}$, and $\dot{\varepsilon}_{min}^N$ the minimum true strain rate predicted by the Norton law.

$$S(t) = S_{necking}(1 + N\dot{\varepsilon}_{min}^N (t_{necking} - t))^{1/N} \tag{6}$$

Evolution of necking and homogenous sections, both subjected to the same load, can be expressed by a differential equation by using the same Norton law, Eq. (5), and the volume conservation, Eq. (3). Time integration between $t_{necking}$ and given time t yields:

$$s^N - {s_{necking}}^N = S^N - {S_{necking}}^N \tag{7}$$

To include the softening behaviour in the model the following flow rule was used; here, ε_{min} is the true strain at minimum true strain rate reached at $t = t_{min}$:

$$\dot{\varepsilon} = C(\sigma^{eng})^N \exp(k(\varepsilon - \varepsilon_{min})) \tag{8}$$

Using the same procedure as before, the homogenous section and relationship between the necking and homogenous section become respectively:

$$S(t) = S_{min}(1 + k\dot{\varepsilon}_{min}^N (t_{min} - t))^{1/k} \tag{9}$$

$$s^k - s_{min}{}^k = S^k - S_{min}{}^k \quad (10)$$

For each temperature, parameters (k, ε_{min}) vary with creep lifetime. For the sake of simplicity, single values were chosen at each temperature for the best agreement between experimental and predicted strain curves (Eq. (9)). Thus, (k, ε_{min}) are taken as (35, 2%) at 500 and 550°C, and (35, 1.8%) at 600°C.

Evolution of the necking section predicted by the model without softening starts at the predicted necking onset. The one using the viscoplastic softening law starts at time t_{min} taken on experimental creep curves when the strain reaches ε_{min}. Both models require the knowledge of the difference in cross-section between the homogenous and necking parts at the predicted necking onset, $\delta S_{necking}$ (= $S_{necking} - s_{necking}$). This parameter is supposed to be equal to the variation in section induced by initial roughness on the specimen surface i.e. a maximum variation of 20μm in diameter, δD. To evaluate the sensitivity of model predictions to this parameter, various values of δD are used to evaluate $\delta S_{necking}$: 1, 10, 20, 50 and 100μm.

The fracture criterion is usually defined as the ratio of the final necking section to the initial cross section ($r_c = s_{necking}/ S_{initial}$). For creep tests at temperatures between 500 and 600°C on Grade 91, r_c ranges between 20 and 80%. Using the fracture criterion r_c = 20%, the predicted lifetime can be deduced from Eqs. (9-10). By varying δD in 1-20μm range (see below), ε_{min} in 0.6-3% range and t_{min}/ t_R in 0.2-0.5 range, two bound laws are finally deduced from the necking model including the softening behaviour. In these equations, k increases with decreasing minimum creep rate (Eq. (2)):

lower bound: $t_{Rinf} = 1.25 \times 0.9899^k / k\dot{\varepsilon}_{min}$ (11)

upper bound: $t_{Rsup} = 2 / k\dot{\varepsilon}_{min}$ (12)

RESULTS AND DISCUSSIONS

Whatever the flow rule considered, lifetimes predicted by the necking model vary by less than 10% when δD ranges in 1-20μm. For both models, times predicted at a reduction of 20% and 80% in cross-section differ by less than 10% (Fig. 5a). Thus, model predictions are not significantly sensitive to the values of $\delta S_{necking}$ and δD. The model including softening predicts fracture earlier than the model without softening. Evolution of the necking section predicted by this model is slow and quickly accelerates only before fracture. This is in agreement with experimental measurements during the interrupted test (Fig. 2b).

From Fig. 5b, the necking model without softening overestimates lifetimes by less than 50% only for creep lifetimes lower than 60×10^3h at 500°C. Predictions using the necking model including softening differ from experimental results by less than 20% for all tests at 500-600°C, except for the one lasting 94×10^3h at 600°C (50%). Considering an experimental scatter of 50% [5], the necking model including softening seems to predict lifetimes correctly.

Fig. 6a compares the evolution of the necking section (predicted by the model including softening) to experimental measurements. Good agreement is found until 75% of the interrupted test lifetime. By considering again the experimental scatter in lifetime (33 vs. 46h in the present data), this prediction seems to be in satisfactory agreement with experiment.

Lifetimes predicted by Eqs. (11-12) are plotted in Fig. 6b. Experimental lifetimes of a large number of tempered martensitic materials are bounded by the lower and upper predictions. The lower bound law is a Monkman-Grant type adding necking. It correctly predicts only lifetimes of short-term creep tests. The upper bound law is a Monkman-Grant relationship. It correctly predicts long lifetimes up to 200×10^3h at 500-700°C.

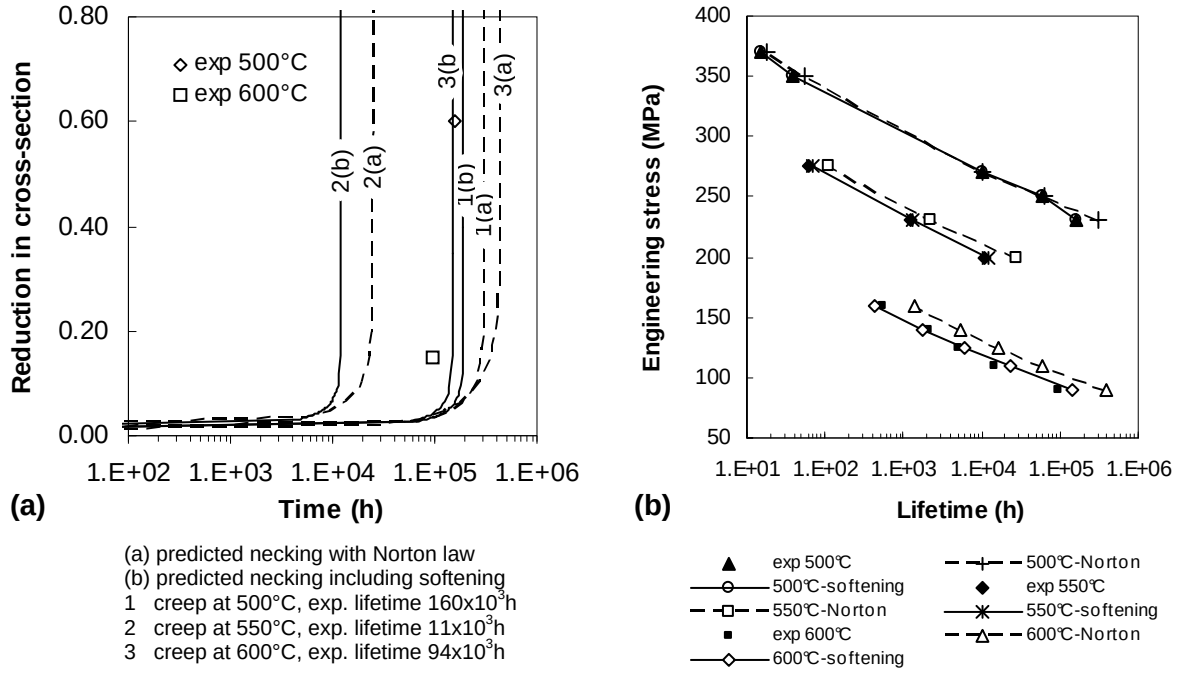

(a) predicted necking with Norton law
(b) predicted necking including softening
1 creep at 500°C, exp. lifetime $160x10^3$h
2 creep at 550°C, exp. lifetime $11x10^3$h
3 creep at 600°C, exp. lifetime $94x10^3$h

Fig. 5: (a) Predicted reduction in cross-section, (b) lifetimes predicted by the necking model either without ("Norton") or with softening, compared to experimental data ("exp").

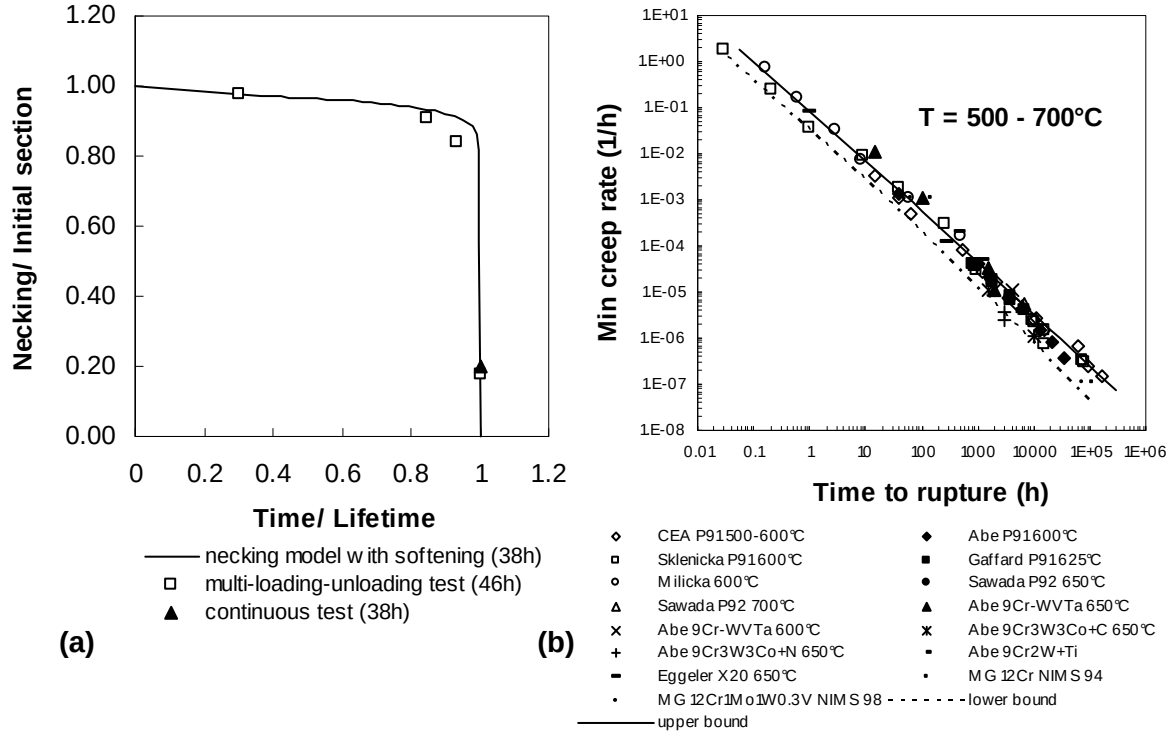

Fig. 6: (a) Necking section evolution for creep test at 500°C and 350MPa. (b) lifetimes predicted by Eqs. (11-12) for a large number of tempered martensitic materials (references are given in [3,11]).

CONCLUSIONS

The necking model with no softening correctly predicts creep lifetimes of Grade 91 lower than 60×10^3h at 500°C. The necking model including temperature-dependent softening correctly predicts lifetimes up to 160×10^3h at 500°C and 94×10^3h at 600°C. The model is stable with respect to the initial variation in specimen diameter and the failure criterion. It predicts evolution of necking in agreement with measurements from an interrupted test.

Lower and upper bound curves describing lifetime vs. minimum creep rate are derived from the model with temperature- and load-dependent softening. The lower bound, taking necking into account, correctly predicts short creep lifetimes. The upper bound (with no necking) correctly predicts long lifetimes. Experimental lifetimes of a number of tempered martensitic materials up to 200×10^3h at 500-700°C are bounded by lower and upper predictions.

REFERENCES

[1] Vaillant, J.C.; Vandenberghe, B.; Hahn, B.; Heuser, H.; Jochum, C.:
T/P23, 24, 911 and 92: New grades for advanced coal-fired–Properties and experience
International Journal of Pressure Vessels and Piping 85 (2008), pp. 38-46

[2] Hoff, N.J.:
The necking and the rupture of rods subjected to constant tensile loads
Journal Applied Mechanics 20 (1953), No. 1, pp. 105-108

[3] Haney, E. M.; Dalle, F.; Sauzay, M.; Vincent, L.; Tournié, I.; Allais, L.; Fournier, B.:
Macroscopic results of long-term creep on a modified 9Cr-1Mo steel
Materials Science & Engineering A 510-511 (2009), pp. 99-103

[4] Eggeler, G.; Earthman, J.C; Nilsvang, N.:
Microstructural study of creep rupture in a 12% chromium ferritic steel
Acta Metallurgica 37 (1989), pp. 49-60

[5] Masuyama, F.:
Hardness models for creep life assessment of high strength martensitic steels.
Material Science & Engineering A 510-511 (2008), pp. 154-157

[6] Hart, E.W.:
Theory of the tensile test
Acta Metallurgica 15 (1957), pp. 351-355

[7] Lemaitre J.; Chaboche J.L.:
Mechanics of solid materials.
Cambridge University Press (1994).

[8] Straub, S.; Meier, M.; Ostermann, J.; Blum, W.:
Development of microstructure and strengthening in ferritic steel X20CrMoV 12 1 at 823K during long-term creep tests and during annealing
VGB Kraftwerkstechnik (1993), pp. 646-653

[9] Gaffard, V.; Besson, J.; Gourgues-Lorenzon, A.F.:
Creep failure model of a tempered martensitic stainless steel integrating multiple deformation and damage mechanisms.
International Journal of Fracture 133 (2005), p.p. 139-166.

[10] Abe, F.; Horiuchi, T.; Taneike, M.; Kimura, K.; Muneki, S.; Igarahi, M.;
Creep strain behaviour during microstructure evolution in tempered martensitic avanced 9Cr Steels.
Creep Resistant Metallic Materials, Prague, Czech Republic (2001), pp. 16-25.

[11] Abe, F:
Stress to produce a minimum creep rate of 10^{-5}%/h and stress to cause rupture at 10^5h for ferritic and austenitic steels and superalloys.
International Journal of Pressure Vessels and Piping 85 (2008), pp. 99-107.

Corresponding author: rattanak.lim@cea.fr